Temporal Processing in the Olfactory System: Can We See a Smell?

David H. Gire[1,7], **Diego Restrepo**[2,*,7], **Terrence J. Sejnowski**[3,4], **Charles Greer**[5], **Juan A. De Carlos**[6], and **Laura Lopez-Mascaraque**[6]

[1]Molecular and Cellular Biology, and Center for Brain Science, Harvard University, Cambridge, MA 02138, USA

[2]Department of Cell and Developmental Biology, Rocky Mountain Taste and Smell Center and Neuroscience Program, University of Colorado Medical School, Aurora, CO 80045, USA

[3]Howard Hughes Medical Institute, Computational Neurobiology Laboratory, Salk Institute, La Jolla, CA 92037, USA

[4]Division of Biological Sciences, University of California San Diego, La Jolla, CA 92093, USA

[5]Department of Neurosurgery and Neurobiology and Interdepartmental Neuroscience Program, Yale University School of Medicine, New Haven, CT 06520, USA

[6]Instituto Cajal, CSIC, 28002-Madrid, Spain

Abstract

Sensory processing circuits in the visual and olfactory systems receive input from complex, rapidly changing environments. Although patterns of light and plumes of odor create different distributions of activity in the retina and olfactory bulb, both structures use what appears on the surface similar temporal coding strategies to convey information to higher areas in the brain. We compare temporal coding in the early stages of the olfactory and visual systems, highlighting recent progress in understanding the role of time in olfactory coding during active sensing by behaving animals. We also examine studies that address the divergent circuit mechanisms that generate temporal codes in the two systems, and find that they provide physiological information directly related to functional questions raised by neuroanatomical studies of Ramon y Cajal over a century ago. Consideration of differences in neural activity in sensory systems contributes to generating new approaches to understand signal processing.

For over a hundred years, comparing and contrasting olfaction and vision has yielded important insights into their structural-functional relationships. Indeed, in 1891, Santiago Ramón y Cajal made a thorough neuroanatomical comparison of the visual and olfactory systems in several species ranging from fish to human (Cajal, 1891). Cajal concluded that signal flow between the olfactory bulb and cortex was reciprocal and bidirectional (Figure 1, arrows). Centrifugal input to the olfactory bulb is major in all animals, including mammals (Neville and Haberly, 2004; Shepherd et al., 2004), and Cajal speculated that "these centrifugal inputs. may produce in the glomeruli some action indispensable for the regular play of the transmitting mechanism." As seen by the terminal boutons in Figure 1, centrifugal input targets the internal granule cells, and Cajal proposed that these interneurons transfer information from the cortex to the mitral and tufted cells, the primary recipients of

synaptic input from the olfactory sensory neurons (OSNs). Within the last few years, rapid progress has been made in understanding how these well-known connections function to deal with complex, time varying input signals during olfactory processing.

Interestingly, because Cajal's work on the visual systems was focused on birds, he concluded that *both* the visual and olfactory systems transfer information not only from the sensory receptor cells to central brain regions but also through centrifugal feedback from the central processing regions to the first processing regions (compare Figures 1 and 2). Yet, later work revealed that centrifugal feedback to retina in mammals is relatively minor (Wilson and Lindstrom, 2011).

Here, we consider the olfactory system relative to the visual system and ask if these two sensory modalities demonstrate converging or widely different coding principles. In particular, we raise instructive differences between the two systems regarding the dimensionality of the signals for system processing, discuss findings for fine-scale temporal coding and synchrony used in olfactory function by awake animals, cortical network architecture supporting processing of such fine-scale spike timing, and centrifugal projections from olfactory cortex that play a role in controlling this timing. Finally, we examine the energetic constraints within which both the olfactory and visual systems operate and show how spike timing may be employed in early sensory processing to most efficiently transmit relevant information. This review focuses on rodent olfactory systems in the mouse and rat where understanding of the role of temporal processing has recently progressed dramatically. These studies are compared to visual studies in mammals that have high visual acuity (primates and cats, for example) as well as to studies in in vitro preparations that have extensively defined basic circuit properties of the retina.

Organization of the Mammalian Olfactory System

The olfactory bulb, the first processing center for olfactory information in the brain, has been likened to the retina in the visual system; a similarity noted by Cajal (compare Figures 1 and 2, and the circuit diagrams in Figure 3). Both the retina and the olfactory bulb exhibit circuitry that supports extensive inhibitory lateral interactions before the information is transmitted to the rest of the brain (Gollisch and Meister, 2010; Mori and Shepherd, 1994; Shepherd et al., 2004). However, there are clear differences. The transduction pathways downstream of the G protein-coupled sensory receptors are distinct (Burns and Baylor, 2001; Ma, 2010; Munger et al., 2009). While visual receptors are embedded in the retina, the sensory receptors for olfaction are located peripheral to the olfactory bulb in the olfactory epithelium, a sheet of tissue within the nasal cavity. The input that the two systems receive is also quite different, with two-dimensional nearest-neighbor spatial correlations present in visual input that appear to be largely absent in olfactory sensory input to the olfactory bulb (Figure 3; Soucy et al., 2009).

Mitral and tufted (MT) cells are the output neurons of the olfactory bulb. Each MT cell receives input from OSNs within a spherical structure of neuropil called a glomerulus, where the axons from OSNs expressing only 1 odorant receptor (out of ~1,200 different receptors) converge (Figure 1; Mori and Sakano, 2011; Shepherd et al., 2004). Such an arrangement restricts the excitatory input for an individual MT to OSNs expressing the same olfactory receptor so that each glomerulus-specific population of MT cells can be thought of as an independent channel of molecular information. Similar to the retina, processing of signals within the olfactory bulb takes place through local circuit axodendritic and dendrodendritic interactions, as well as through electrical coupling. In the olfactory bulb, electrical coupling has been physiologically demonstrated within and between classes of excitatory neurons (Christie et al., 2005; Hayar et al., 2005; Lowe, 2003) and inhibitory

processing in the olfactory bulb is mediated by interneurons, the periglomerular and granule cells (reviewed by Mori and Sakano, 2011; Schoppa and Urban, 2003). Mitral and tufted cells display different but somewhat overlapping projection patterns to numerous downstream structures, including the anterior olfactory nucleus, olfactory tubercle, the olfactory (piriform) cortex, amygdala, and entorhinal cortex (Nagayama et al., 2010; Shepherd et al., 2004).

From this circuitry it emerges that the MT cells of the olfactory bulb are one synapse from the periphery and project directly to integrative structures such as the olfactory (piriform) cortex and amygdala (Cajal, 1904; Shepherd et al., 2004; Figure 1). MT cells have thus classically appeared to form a single-neuron bridge between peripheral receptor neuron input and associative integration of that input. In contrast, retinal ganglion cells (RGCs), which project from the retina to downstream visual structures such as thalamus and superior colliculus, do not receive direct sensory neuron input, but instead receive input from bipolar cells that in turn have synaptic inputs from cone visual receptor cells (Cajal, 1904; Sterling and Demb, 2004) (Figure 2; circuit diagram in Figure 3). Interestingly, while it remains somewhat controversial, recent work indicates that mitral cells (MC) are only partially activated by direct input from OSNs and take the majority of their excitation from external tufted cells in the glomerulus (Gire et al., 2012; Najac et al., 2011). Such results suggest that the circuitry of the retina and the MC circuitry in olfactory bulbs are more similar than previously thought. Thus, external tufted cells communicate to olfactory bulb output MCs, thereby functioning somewhat like bipolar cells of the retina that communicate to retina output ganglion cells (Figure 3).

Unlike the visual system, wherein the retinal output flows to cortex primarily via a relay in the lateral geniculate nucleus of the thalamus (Sterling and Demb, 2004), olfactory information bypasses the thalamus and—after an initial relay in the olfactory bulb—is sent directly to the olfactory (piriform) cortex (Neville and Haberly, 2004). Importantly, connectivity of piriform cortex suggests that it functions as "association cortex" in other sensory systems (Johnson et al., 2000). In addition, recent work has demonstrated that optogenetic activation of small subsets of piriform neurons can be used for decision making in the absence of olfactory input, indicating that activity in piriform cortex does indeed convey information that could be relevant for olfactory decision making (Choi et al., 2011). However, there is also direct output from olfactory bulb MCs to entorhinal cortex (Sosulski et al., 2011; Vanderwolf, 1992) that mediates functional coupling from bulb to hippocampus in the β frequency range during olfactory learning (Gourévitch et al., 2010) and lesions of the ventral hippocampus affect working memory for odor information (Kesner et al., 2011).

Because the anatomical link between the olfactory bulb and cortex to the hippocampus through entorhinal cortex was found to be strong and because hippocampus was larger relative to the entire brain in macrosmatic animals, Cajal speculated that the hippocampus was part of the olfactory system (Cajal, 1901). This relationship between the olfactory system and hippocampus is currently not well understood, and in future studies it will be particularly important to compare the role of piriform cortex to circuits linking the olfactory bulb directly to entorhinal cortex in olfactory learning, working memory and olfactory-motor coupling (Xu and Wilson, 2012). Indeed, understanding this input to hippocampus will likely be useful for future understanding of signal processing in this structure.

Since a majority of work on postsynaptic processing of MT output has been conducted in the piriform cortex, we will focus here on the mechanisms of MT communication from the olfactory bulb to the piriform cortex. We will address olfactory bulb to piriform projections in enough detail to provide adequate context for an understanding of the temporal processing of olfactory signals. We suggest the reader consult recent reviews for a comprehensive

discussion of the piriform cortex (Isaacson, 2010; Wilson and Sullivan, 2011) and signal processing and input to the glomerular layer of the olfactory bulb (Cleland, 2010; Linster and Cleland, 2009; Mori and Sakano, 2011; Wachowiak and Shipley, 2006), as well as a general discussion of olfactory temporal coding (Bathellier et al., 2010).

The piriform cortex is composed of three layers. Input from MT cell axons terminates on the distal dendrites of piriform cortex pyramidal cells (PCs) in layer Ia. Layer Ib includes local circuit synapses and interneurons while layers II and III contain the cell bodies of PCs (Neville and Haberly, 2004). Individual PCs receive input from MTs scattered throughout the olfactory bulb (Apicella et al., 2010; Davison and Ehlers, 2011; Miyamichi et al., 2011; Wilson, 2001) and the axons of individual MTs branch extensively throughout piriform cortex (Ghosh et al., 2011; Sosulski et al., 2011). Given this connectivity, PCs receive input from a diverse population of odorant receptors and therefore could function as combinatorial sensors (Haberly, 2001; Mori et al., 1999; Wilson and Sullivan, 2011) that integrate activity resulting from activation of broad swaths of molecularly defined OSNs. Consistent with this hypothesis, cross-habituation studies suggest that PCs respond to combinations of odor molecular features, and not single molecular features as do MT cells (Wilson et al., 2000; Wilson and Rennaker, 2010). Further, activation of MT cells across a wide area of the olfactory bulb is required to drive PCs to spike (Arenkiel et al., 2007; Davison and Ehlers, 2011). Finally, significant sparsening of odor responses is thought to occur between bulb and cortex (Poo and Isaacson, 2009), suggesting that in addition to integrating input from multiple glomeruli, mechanisms are in place to filter incoming bulbar input onto PCs. Importantly, piriform cortex, particularly posterior piriform cortex, receives significant input from the rest of the brain (Illig, 2005; Maier et al., 2012).

Feedforward Inhibition and Coincidence Detection in Piriform Cortex

Piriform cortex exhibits strong sensory-evoked inhibition (Poo and Isaacson, 2009), which serves to narrow the temporal window during which MT input can be effectively integrated (Luna and Schoppa, 2008; Stokes and Isaacson, 2010). Di-synaptic feedforward inhibition acts on PCs in as little as 2 ms following MT cell spike input. This inhibition is well suited to truncate sensory input, as it occurs in the distal dendritic arbor, where MT axons terminate (Stokes and Isaacson, 2010). Disynaptic inhibition onto PC dendrites is mediated by layer 1a interneurons (neurogliaform and horizontal cells; see Suzuki and Bekkers, 2012), which are reliably activated by MT cell axons due to a larger number of axons targeting these cells as well as a higher release probability for MT to interneuron synapses in contrast to MT to PC connections (Stokes and Isaacson, 2010).

During a burst of action potentials from MT cells, disynaptic feedforward inhibition to the dendrites depresses, and polysynaptic feedback inhibition targeted to the PC soma begins to dominate during later spikes in the train. This form of inhibition is short latency following MT cell input (5–10 ms; Luna and Schoppa, 2008), and has been suggested to originate primarily from interneurons driven by PC cell spikes (Stokes and Isaacson, 2010).

Although PCs have active dendritic conductances (Bathellier et al., 2009), inhibition by interneurons sets a short temporal window for integration of MT input by PCs. Indeed, elimination of inhibition greatly expands temporal integration in PCs, such that integration is then only limited by the membrane time constant of the PC (Luna and Schoppa, 2008). Further, MT input is broadly spread across the distal dendritic arbor of each neuron and does not appear capable of causing dendritic spikes (Bathellier et al., 2009). This is in marked contrast to other neural systems, where clustered input onto active dendrites supra-linearly amplifies near-simultaneous synaptic input to cause dendritic spikes (Ariav et al., 2003).

Taken together, studies regarding the temporal integration of input within the piriform cortex suggest that MT spikes will most effectively drive PCs if they are synchronized on a very short timescale (<2 ms). Failing this, later spikes during barrages of input from MT cells could overcome this rapid inhibition. Even under these conditions, however, polysynaptic inhibition within the piriform functions to limit the window for temporal integration in PCs to 5–10 ms. The rapid time course of inhibition in the piriform cortex suggests that individual PCs act primarily as coincidence detectors and integrate MT input over just a few milliseconds. We will next address the nature of spike output in MT cells and review literature suggesting that MT cell output in awake animals is well suited to drive PCs under these conditions.

Temporal Precision, Phase Locking, and Efficient Population Coding in MT Cells

In awake rodents, a large number of glomeruli are activated by single odorants (Johnson and Leon, 2007; Mori et al., 2006; Salcedo et al., 2005; Vincis et al., 2012). During dense glomerular activation a relatively large number of MT cells respond to odor input by *transiently* locking their spiking to the ongoing respiratory rhythm (Figure 4; Bhalla and Bower, 1997; Chaput, 1986; Cury and Uchida, 2010; Gschwend et al., 2012; Pager, 1985; Shusterman et al., 2011). For example, Shusterman et al. (2011) showed that approximately half of MT-odor pairs (59%) show a phasic sniff-locked response. Previous theoretical work (Hopfield, 1995) as well as experimental work in anesthetized rodents (Bathellier et al., 2008; Cang and Isaacson, 2003; Margie and Schaefer, 2003; reviewed by (Schaefer and Margie, 2007) has suggested that such temporal coding could be a plausible method for transmitting information regarding odor identity and concentration in the olfactory system. In the visual system, this coding strategy has been demonstrated to transmit information in RGCs from salamander retina, and suggested to occur following fixation during saccadic eye movements (Figure 4; and see Gollisch and Meister, 2008). However, its utility in the olfactory system during active sampling was not extensively explored until recent experiments in awake rodents. Dense phase locking of MT cells to respiration in awake rodents was found to be sensitive to the identity of the odor (Cury and Uchida, 2010; Shusterman et al., 2011) and to exhibit high reliability, with a trial-to-trial jitter during identical odors of 12 ms (Shusterman et al., 2011; Smear et al., 2011). Further, it can occur without an increase in spike rate averaged over the respiratory cycle (Cury and Uchida, 2010; Gschwend et al., 2012; Shusterman et al., 2011; Smear et al., 2011). This phase-locked sensory-evoked activity in large numbers of MTs is likely energetically favorable, as it conveys information without the metabolic demand caused by a long lasting increase in spike activity (Attwell and Laughlin, 2001).

By employing an energy efficient coding scheme, more neurons can be actively used in coding for the same metabolic cost, which reduces the number of "silent" neurons (and thus the redundancy of the population; see Laughlin, 2001; Laughlin and Sejnowski, 2003) and increases the representational capacity of the network (Abbott et al., 1996; Rolls et al., 1997). At the extreme, such a coding mechanism could allow for involvement of a majority of MT cells in each odor representation (a dense distributed representation; see Rolls et al., 1997). In this context, it is interesting that recent reports suggest that each of the glomeruli in the olfactory bulb of mice are innervated by roughly 10–25 mitral cells—redundancy in coding may help reduce the number of required functional units dedicated to any one molecularly defined odorant receptor (Miyamichi et al., 2011; Richard et al., 2010; Sosulski et al., 2011). Incidentally, estimates of the number of glomeruli range in mice from 1,800–3,700 (Richard et al., 2010; Royet et al., 1988).

This high percentage of phase-locked responses is in sharp contrast to the relatively sparse responses observed in awake animals when only changes in firing rate are considered independent of phase locking to sniffing (Davison and Katz, 2007; Doucette and Restrepo, 2008; Gschwend et al., 2012; Kay and Laurent, 1999; Rinberg et al., 2006), which may be a more metabolically demanding coding method. Until recently, this sparse rate code was the predominant code examined in olfaction, which led to the conclusion that the olfactory bulb utilizes sparse coding to transmit information in the awake state (Gschwend et al., 2012; Rinberg et al., 2006). With new evidence suggesting that sniff-locked spikes represent a dense distributed code in the bulb, coding in the early olfactory system must be re-examined with a particular attention paid to responses under different behavioral context.

Dense distributed coding involves features that are advantageous to early olfactory processing. Chief among these advantages, a distributed code allows for the greatest amount of representational capacity across the network (Rolls et al., 1997). This would be useful in olfaction, as the high dimensionality of the input requires a large capacity to faithfully encode the stimulus. Given the unpredictable connections possible between an arbitrary combination of odors and a behavioral response, faithfully encoding the high dimensionality of olfactory input within the population of MT cells may be necessary, as the system cannot predict a priori which dimensions (i.e., olfactory receptor activation) will be important in distinguishing one behavioral cue from another. Additionally, the loss of parts of the network does not compromise the ability to discriminate between network states in a distributed coding scheme, and, in fact, massive bulbar lesions do not impair odor detection or discrimination during some tasks (Bisulco and Slotnick, 2003; Slotnick and Bodyak, 2002). While dense distributed codes involving spike rate are thought to be energetically wasteful (Levy and Baxter, 1996), the olfactory bulb appears to use the phase of spikes relative to inhalation to encode the high dimensionality of olfactory input without greatly increasing spike rate and energy consumption in MT cells.

Estimates of the number of MT cells needed to accurately discriminate odors using a sniff-phase-based code range from a low of 5–25 (90% classification success rate with 25 randomly chosen neurons across five odors; Shusterman et al., 2011) to more than 200 (Cury and Uchida, 2010). Differences in these estimates could arise from two different experimental paradigms, with one study using head-restrained mice (Shusterman et al., 2011) and the other, freely moving rats (Cury and Uchida, 2010). In either case, the number of neurons active during odor application largely exceeds the number of neurons absolutely needed to accurately perform odor discrimination. This disparity suggests that either simple discrimination tasks are not probing the limits of olfactory coding, and/or that this form of coding exhibits a level of redundancy. While redundancy is usually detrimental to efficient coding, it may be necessary in the case of olfactory coding, given that MT cells project in parallel to multiple central structures (e.g., cortex and amygdala) that may combine and process bulbar output differently (Ghosh et al., 2011; Sosulski et al., 2011).

Whether the precise timing of MT spikes relative to sniffing conveys information directly from the periphery (i.e., timing of OSN spiking), or instead provides "extra bandwidth" to convey additional information not directly locked to the temporal aspect of the stimulus (as in vision; see Butts et al., 2007) remains an open question. Although MTs have been shown to reliably respond to precisely timed optogenetic OSN activation (Smear et al., 2011) the output of mammalian OSNs during odor stimulation does not appear to be obviously related to odor input dynamics or concentration (Ghatpande and Reisert, 2011). Additionally, simultaneously recorded MTs associated with a single, receptor-specific glomerulus show different spike timing relative to sniffing during odors (Dhawale et al., 2010). Finally, a recent study by Miura and coworkers shows that information on odor quality carried by

timing of spikes in MT cells is transformed into a rate code in piriform cortex PCs that involves transient bursts of spikes locked to sniff (Miura et al., 2012).

Consequences of the Differences in the Dimensionality of Visual and Olfactory Sensory Inputs

Why does the olfactory system employ such dense representations of sensory input at the earliest stages of processing, while at this same stage the visual system efficiently employs a relatively sparse coding scheme? The visual system can take advantage of spatial correlations in natural visual scenes to attain efficient coding in the output of the retina by eliminating redundancies before transmission to cortex (Figure 3; Dan et al., 1996; Doi et al., 2012; Olshausen and Field, 1996; Sincich et al., 2009). Indeed, recent studies reveal that in the retina the transfer of information of natural images from cones to RGCs is ~80% efficient (Doi et al., 2012). This high efficiency is key to a system that is constrained in its transfer of information from the RGCs to the lateral geniculate nucleus of the thalamus by a physically restricted small number of axons. High efficiency information transfer is achieved by optimal projective fields for transfer of information from the cones to the RGCs (Doi et al., 2012). Thus, the visual system uses the well-defined spatial relationship of input to cones to transmit information in an efficient manner.

In sharp contrast, the relationship between information conveyed by different olfactory receptors is not necessarily pre-defined for novel multimolecular odors. Moreover, due to its high dimensionality, the physiochemical properties of odors cannot be neatly mapped onto the two dimensional laminar layers of the MOB and odor input will inevitably become fragmented as this dimensionality is necessarily reduced (Figure 3; Cleland and Sethupathy, 2006). Therefore, the optimization of information transfer from specific glomeruli to the olfactory bulb and beyond is a complicated problem. The processing of a smell involves an input possibly entailing hundreds of dimensions generated when a time varying chemical stimulus interacts with hundreds of different olfactory receptor types (Buck and Axel, 1991; Franks et al., 2011; Godfrey et al., 2004; Zhang and Firestein, 2002).

Since olfactory receptors detect molecular features within an odorant (Araneda and Firestein, 2006; Nara et al., 2011; Saito et al., 2009), even artificial single odors such as isoamyl acetate (banana) stimulate numerous receptor types in a time-varying input that results in activation of a subset of the 1,800–3,700 olfactory glomeruli in complicated glomerular maps that are partially overlapping for different odors (Johnson and Leon, 2007; Mori et al., 2006; Soucy et al., 2009; Spors et al., 2006; Vincis et al., 2012). In addition, natural odors such as mouse urine that convey information on the animal's genetic makeup, health and status (Hurst and Beynon, 2004; Kwak et al., 2010) incorporate hundreds of volatile molecules (Kwak et al., 2008) and also elicit glomerular odor maps that are surprisingly as complex as maps for single odor molecules (Schaefer et al., 2002). Moreover, the olfactory system cannot simply focus on a predefined subset of its input because novel chemosensory objects may stimulate a new subset of receptors that could signal a potentially important environmental cue. Thus, the olfactory system must remain highly flexible in its processing of its input.

Because of this need for high flexibility, the olfactory system appears to deal with its first level of input in a very different manner than the visual system. In the mouse retina, there are 22 types of ganglion cells that tile the visual field, each type encoding a different spatiotemporal pattern on the array of photoreceptors. This is a much lower dimensionality than the coding dimensionality in the olfactory bulb; however, the 2D arrays of ganglion cells provide the visual cortex with spatial coding dimensions that are not found in the olfactory bulb. One notable, potentially significant, difference between the olfactory and

visual systems is the generation of new interneurons in the adult olfactory bulb, and not in the adult retina. In the bulb new granule cells and periglomerular cells are generated by the subventricular zone (SVZ) and the rostral migratory stream (RMS) in the adult mammal, although it is not clear whether this takes place in human (Altman and Das, 1965; Alvarez-Buylla and Lim, 2004; Bergmann et al., 2012; Eriksson et al., 1998; Ming and Song, 2005; Zhao et al., 2008). Importantly, these new cells appear to be necessary for signal processing in a subset of challenging olfactory discrimination learning tasks (Alonso et al., 2012; Bardy et al., 2010). Indeed, recent optogenetic studies indicate that activation of adult-born olfactory bulb neurons facilitates learning and memory (Alonso et al., 2012). Interestingly, gamma1 (40 Hz) activation of newly generated granule cells—a frequency likely key for circuits involved in olfactory learning (Kay et al., 2009)—but not 10 Hz activation resulted in enhanced learning and memory. Future studies are necessary to solidify whether generation of new neurons impacts odor discrimination and to explore the frequency range for signal processing that may be modified by the newly generated granule cell neurons during learning of difficult odor discrimination (Beshel et al., 2007; Kay et al., 2009). In comparison, there is no generation of neurons in the retina in the adult, but activation of retinal neuronal generation is being explored to treat macular degeneration (Fang et al., 2013). Likely the visual system has optimized retinal processing without a need to generate new neurons in the adult because although this input is extremely complex, signal processing can be performed based on the fixed relationship of input from different points in the two dimensional retinal space. In contrast, because the olfactory system has the challenging task of bringing together information from over ~1,200 different dimensions whose relationships are not fixed the system likely re-wires the circuit in the olfactory bulb to optimize the learning of behaviorally relevant novel combinations of these dimensions (see Figure 3).

Synchrony and Multiplexing in Mammalian Olfaction

While sniff-locked spike timing in MTs can convey temporal information related to odor identity, recent work has shown that precise sub-millisecond synchrony between MTs conveys information related to the reward contingency associated with a given odor, rather than temporal cues associated with the identity of that odor (Doucette et al., 2011). During a single training session MT cells show increased synchronous firing in response to an odor associated with a reward. This synchrony occurs between a small fraction of spikes in MT cells (on average 0.9% of spikes are synchronized between any two MT cells, though some pairs show no synchrony) and occurs even between widely separated MT cells (from 200 μm to >1 mm). Figure 5 illustrates an example of this fast synchrony as well as a plausible mechanism that could support it within the olfactory bulb. Synchronized spikes can be used to discriminate between a rewarded and unrewarded odor and carry information that is not available within single neuron rate coding alone (Doucette et al., 2011; Figure 4).

Precise synchrony thus appears to be a coding mechanism that operates concurrently with rate and sniff-locked coding, carrying information regarding the association between an odor and reward. This form of coding, with spikes considered at different timescales of a response signaling diverse features of a stimulus, is called multiplexing. Multiplexing has been suggested to be common across multiple sensory systems (reviewed by Panzeri et al., 2010). In addition to MT cells in mammalian systems, neurons within the zebra fish olfactory bulb have been shown to employ a multiplexed code, with rate responses being indicative of the identity of an odor while synchronized spikes in phase with the LFP simultaneously code for the category of the odor (Friedrich et al., 2004). Interestingly, in zebrafish the dorsal telencephalon (Dp), a target of the olfactory bulb analogous to olfactory cortex, is largely insensitive to oscillatory synchrony, while phase-locked LFP oscillations were detected in a different area in central telencephalon that likely processes synchrony of

MC ensembles (Blumhagen et al., 2011). Thus, both synchronized and unsynchronized firing may carry different streams of information.

Importantly, synchrony on fast timescales (<1 ms) is ideally suited to transmit information from the olfactory bulb to the cortex, as feedforward inhibition operates on this timescale (Stokes and Isaacson, 2010). That this synchrony can occur between cells that are any distance apart in the olfactory bulb allows for arbitrary combinations of MTs responding to activation of various receptors to become synchronized (Figure 5). This feature is of particular use in olfaction, since arbitrary combinations of odors may signal behaviorally relevant events. Thus, the mammalian olfactory system could employ precise synchrony to preferentially transmit information regarding the presence of behaviorally relevant odors past rapid feedforward inhibition within the cortex. Finally, correlation and synchrony play a role in the visual system. In the retina the cone accounts for most of the noise and correlations in the retinal output and constrains how higher centers exploit signals carried by parallel visual pathways (Ala-Laurila et al., 2011). In addition, synchrony in thalamocortical inputs in the visual system would maximize reliability of upstream information transfer (Wang et al., 2010).

Synchrony and Multiplexing in Mammalian Vision

One million ganglion cells in the retina drive 100 million cells in the primary visual cortex via relay cells in the thalamus. However, the afferents of the relay cells on layer 4 spiny stellate simple cells constitute only ~5% of the synapses, with most of the others arising from other cortical neurons, which are spontaneously active. In a detailed biophysical model of the spiny stellate cell, the reliability of transmission into the cortex increased steeply between 20 and 40 synchronous thalamic inputs in a time window of 5 ms, when the reliability per spike was most energetically efficient (Wang et al., 2010). Since each relay cell makes 2–10 synapses on a spiny stellate cell, synchrony in only 4–8 relay cells are needed. The optimal range of synchronous inputs was influenced by the balance of background excitation and inhibition in the cortex, and feedback from the cortex to the thalamus.

Thus, as in the olfactory system, information in a population of neurons is efficiently encoded to the cortex by converging synchronous spikes. Far more spikes would be needed to achieve the same level of reliability of transmission without synchrony. This efficiency though requires a high level of precision in the projections from the retina to the lateral geniculate nucleus to preserve the topographical map from the retina, and convergence of the relay cells onto spiny stellate cells to create spatial features such as orientation tuning in cortical neurons (Figure 5). This requirement may not be necessary for the inputs to piriform cortex, where there is little apparent topographic organization and PCs receive inputs from many different glomeruli.

What Is the Role of Cortical Feedback?

As shown by Cajal, both the olfactory and visual systems have centrifugal feedback (Figures 1 and 2; Cajal, 1891). In the case of the visual system, centrifugal feedback to the retina is limited (with the exception of birds), and its role is not entirely clear but has been suggested to help birds perform rapid search for a predator in the sky (Wilson and Lindstrom, 2011). However, in mammals, there is recent information on the role of the substantial centrifugal feedback from cortex to the lateral geniculate nucleus in the thalamus and in the visual system (Briggs and Usrey, 2009, 2011) and from piriform cortex or anterior olfactory nucleus (AON) to olfactory bulb in the olfactory system (Balu et al., 2007; Boyd et al., 2012; Markopoulos et al., 2012; Strowbridge, 2009), initially investigated by Nakashima et al. (1978).

Interestingly, anatomical studies from Cajal (1901), confirmed by more recent neuroanatomical studies (De Carlos et al., 1989; Matsutani, 2010), indicated that MCs receive direct centrifugal feedback (Figure 6). Importantly, recent studies by the Isaacson and Murthy groups yield information on potential functional and behavioral roles for centrifugal feedback (Boyd et al., 2012; Markopoulos et al., 2012); they show that optogenetically driven activity in the piriform cortex and anterior olfactory nucleus (AON; an olfactory cortical structure separate from the piriform) suppresses odor-evoked excitation of MCs through disynaptic inhibition from inhibitory interneurons, the periglomerular and granule cells (Figure 7). Photoinduced gamma activity in the centrifugal fibers from the piriform cortex strongly inhibits β activity in the olfactory bulb and inhibits odor-induced activation of MCs. Coupled with recent studies showing increased β activity and MC responses to odors elicited by go-no go learning of odor discrimination, these studies suggest cortical feedback could play a role in gating MC firing based upon learned odor-reward associations (Doucette et al., 2011; Martin et al., 2004). Interestingly, steady state MC firing conveys information on odor reward as opposed to odor quality (Doucette et al., 2011; Doucette and Restrepo, 2008). In addition, Markopoulos and coworkers found evidence suggesting that AON feedback axons can also make direct, but very sparse, excitatory connections with MCs. These were weak connections but were able to elicit precisely timed action potentials in moderately activated cells both in precisely controlled slice experiments (Figure 7) and in vivo (Figure 5). Thus, cortical feedback could contribute to the well-known changes in steady state firing in MT cells during olfactory learning, as well as precisely timed synchrony between MT cells (see mechanism in Figure 5; Doucette et al., 2011; Doucette and Restrepo, 2008). Importantly, although steady state MC firing conveys information on odor reward association, changes in firing within the sniff likely conveys information on odor quality (Cury and Uchida, 2010; Shusterman et al., 2011). Understanding how information on odor valence and odor quality is conveyed by neurons in the olfactory system requires future work.

Conclusions

In this review, we have focused on temporal processing in mammalian olfaction, and we have discussed the rich repertoire of temporal coding in this system, comparing it to that used by the visual system. This includes multiplexing multiple codes at different timescales, the use of sniff-phase for energy efficient dense distributed coding of odor identity, and the role of precise synchrony in conveying behaviorally relevant information to the cortex. The usage of spike timing in olfaction allows more cells to be brought into the olfactory code at early processing stages, increasing the representational capacity of the system, while more sparsely occurring precisely synchronized spikes transmit behaviorally relevant information to the cortex. Work in invertebrate olfactory systems also suggests an extensive role for temporal processing in chemosensory sensing and learning (see Aldworth and Stopfer, 2012; Cassenaer and Laurent, 2012; Laurent, 2002). This combination of phase coding with synchronization could allow the system to take advantage of dense distributed coding to discriminate between an immense number of odors, while a more sparse code involving synchronized spikes represents associational cues and would have advantages in the context of associational memory and pattern recognition (Olshausen and Field, 2004). Interestingly, while vision employs similar temporal coding strategies, the function of such coding appears to be to efficiently transmit information regarding fixed aspects of the stimulus rather than to flexibly incorporate associational information. Finally, we discussed how centrifugal feedback, known since Cajal's work, but only recently described physiologically, could contribute to temporal coding in olfaction.

A comparison between the studies in the visual system and the olfactory system underscores the relatively poorly characterized functional roles of different olfactory bulb projection

neurons and the circuits they innervate (Asari and Meister, 2012; Field and Chichilnisky, 2007; Sterling and Demb, 2004). In particular, it is known that tufted cells respond to odors in a manner drastically different than mitral cells (Fukunaga et al., 2012; Nagayama et al., 2004) and that tufted and mitral cells innervate different upstream targets (Igarashi et al., 2012; Nagayama et al., 2010). However, these parallel circuits remain poorly defined and not well understood as regards the processing of odors. Indeed, over a hundred years ago Ramon y Cajal was among the first to recognize the substantial difference in axonal projections of mitral and tufted cells to cortical targets (Cajal, 1904). He concluded that it is *probable* that tufted cells innervate the contralateral olfactory bulb ("marcha probable de las corrientes" [Cajal, 1904]), a finding known to be incorrect (Lopez-Mascaraque, 2006; Figure 8). However, it seems reasonable to suggest Cajal's incorrect conclusion regarding a contralateral projection by tufted cells reflects the fact that he was pushing the envelope of structure-function correlates in an attempt to understand the differential involvement of mitral and tufted cell circuits in odor processing. Even now, it is important that Cajal's lead be followed and we continue to push the envelope on the olfactory system. Interestingly, recent findings address where these tufted cell axons actually project and suggest that activation of tufted cells innervating medial and lateral glomeruli targeted by the OSNs expressing the same olfactory receptor are likely to be involved in coding of odorant concentration (Zhou and Belluscio, 2012) and that the mitral cells innervating those glomeruli have different central targets (Imamura et al., 2011).

Compared to the visual system, we know relatively little about the olfactory circuitry and the intricacies of odor processing at different stages of processing in parallel circuits. Thus, Figure 9 shows a drawing by Cajal of a subset of the neurons involved in signal processing in the olfactory bulb. Although we are beginning to understand the involvement of a subset of these cells, such as the Blanes cell (Pressler and Strowbridge, 2006), in signal processing, there is a need for future work with more thorough understanding of the involvement of the different cells in olfactory bulb signal processing (for example the role of tufted cells that send axon colaterals back into the glomerular layer, Figure 9). Future studies are necessary to determine how the subpopulations of MT cells and the circuits they form are involved in odor information processing and cognition. Even less is known about the olfactory features that drive PCs in the piriform cortex, which is being addressed with optical recording techniques and optogenetics (Choi et al., 2011).

Future studies are also key to understand how the centrifugal input into the olfactory bulb described initially by Ramon y Cajal (Cajal, 1891) and recently shown to affect signal processing in the olfactory bulb (Balu et al., 2007; Boyd et al., 2012; Markopoulos et al., 2012; Strowbridge, 2009), affects processing of olfactory information underlying behavior.

Figure 10 shows microphotographs taken from some of Cajal's original preparations of the olfactory bulb, piriform cortex, and retina. These photographs make it clear that tramping from the histological data to formulating hypothetical circuits (the drawings in Figures 1 and 2, Figure 6, and Figures 8 and 9) was not trivial. Advances in our understanding of odor processing via parallel circuits with massive centrifugal feedback has progressed significantly (Figures 3, 4, 5, and 7) and further progress will depend on monitoring and manipulating neurons in both the olfactory bulb and the piriform cortex during olfactory behaviors including discriminative learning.

Finally, throughout this review we have shown that both the olfactory and visual systems employ similar temporal coding strategies to convey information relative to active sampling and to effectively drive their target cells in sensory cortical areas. However, these two systems employ these codes to convey information that is uniquely suited to the processing demands of each system. Thus, since olfactory cues involve (perhaps irreducibly) high

dimensional input to which arbitrary associations may be attached, the olfactory system uses temporal coding to increase its representational capacity and to attach associational significance to arbitrary combinations of its input. Visual cues, on the other hand, occur in predefined spatial relationships to one another. Temporal coding in the visual system is thus used to reduce redundancy and efficiently transmit information between processing stages.

So, can we see a smell? Based upon the work presented throughout this review, one could imagine that a set of spike trains from the olfactory bulb might easily be confused with one from the LGN of the thalamus. On a population level, precisely synchronized spikes would be present, as would phase-locking to ongoing sensory sampling. Would the "meaning" of these temporal features in the code be different? When the visual input from the retina is redirected to the auditory cortex of a cat, it can "see" with its auditory cortex (Sur et al., 1988). A recent study in mouse retina has opened the door to asking whether a mouse can "smell" with its visual cortex. Nirenberg and Pandarinath (2012) introduced ChR2 into the ganglion cells of a mouse lacking photoreceptors and were able to recover visual sensation. However, visual tracking did not occur to a drifting grating when the ganglion cells were presented with the intensity of the grating, but the mice were able to track the grating when it was first passed through the filter of an on-center ganglion cell, which had much stronger temporal modulation. It would be interesting to stimulate the ganglion cells with the pattern of activity from the olfactory bulb, to see whether the mouse could "see a smell."

The complementary consideration of the visual and olfactory systems has been and will continue to be useful. In the past this has been useful to exploring the olfactory system, but future consideration will likely contribute to both fields because considering the differences generates new approaches to understanding sensory processing.

Acknowledgments

References

Abbott LF, Rolls ET, Tovee MJ. Representational capacity of face coding in monkeys. Cereb Cortex. 1996; 6:498–505. [PubMed: 8670675]

Ala-Laurila P, Greschner M, Chichilnisky EJ, Rieke F. Cone photoreceptor contributions to noise and correlations in the retinal output. Nat Neurosci. 2011; 14:1309–1316. [PubMed: 21926983]

Aldworth ZN, Stopfer M. Olfactory coding: tagging and tuning odor-activated synapses for memory. Curr Biol. 2012; 22:R227–R229. [PubMed: 22497937]

Alonso JM, Usrey WM, Reid RC. Precisely correlated firing in cells of the lateral geniculate nucleus. Nature. 1996; 383:815–819. [PubMed: 8893005]

Alonso M, Lepousez G, Sebastien W, Bardy C, Gabellec MM, Torquet N, Lledo PM. Activation of adult-born neurons facilitates learning and memory. Nat Neurosci. 2012; 15:897–904. [PubMed: 22581183]

Altman J, Das GD. Post-natal origin of microneurones in the rat brain. Nature. 1965; 207:953–956. [PubMed: 5886931]

Alvarez-Buylla A, Lim DA. For the long run: maintaining germinal niches in the adult brain. Neuron. 2004; 41:683–686. [PubMed: 15003168]

Apicella A, Yuan Q, Scanziani M, Isaacson JS. Pyramidal cells in piriform cortex receive convergent input from distinct olfactory bulb glomeruli. J Neurosci. 2010; 30:14255–14260. [PubMed: 20962246]

Araneda RC, Firestein S. Adrenergic enhancement of inhibitory transmission in the accessory olfactory bulb. J Neurosci. 2006; 26:3292–3298. [PubMed: 16554479]

Arenkiel BR, Peca J, Davison IG, Feliciano C, Deisseroth K, Augustine GJ, Ehlers MD, Feng G. In vivo light-induced activation of neural circuitry in transgenic mice expressing channelrhodopsin-2. Neuron. 2007; 54:205–218. [PubMed: 17442243]

Ariav G, Polsky A, Schiller J. Submillisecond precision of the input-output transformation function mediated by fast sodium dendritic spikes in basal dendrites of CA1 pyramidal neurons. J Neurosci. 2003; 23:7750–7758. [PubMed: 12944503]

Asari H, Meister M. Divergence of visual channels in the inner retina. Nat Neurosci. 2012; 15:1581–1589. [PubMed: 23086336]

Attwell D, Laughlin SB. An energy budget for signaling in the grey matter of the brain. J Cereb Blood Flow Metab. 2001; 21:1133–1145. [PubMed: 11598490]

Balu R, Pressler RT, Strowbridge BW. Multiple modes of synaptic excitation of olfactory bulb granule cells. J Neurosci. 2007; 27:5621–5632. [PubMed: 17522307]

Bardy C, Alonso M, Bouthour W, Lledo PM. How, when, and where new inhibitory neurons release neurotransmitters in the adult olfactory bulb. J Neurosci. 2010; 30:17023–17034. [PubMed: 21159972]

Bathellier B, Buhl DL, Accolla R, Carleton A. Dynamic ensemble odor coding in the mammalian olfactory bulb: sensory information at different timescales. Neuron. 2008; 57:586–598. [PubMed: 18304487]

Bathellier B, Margrie TW, Larkum ME. Properties of piriform cortex pyramidal cell dendrites: implications for olfactory circuit design. J Neurosci. 2009; 29:12641–12652. [PubMed: 19812339]

Bathellier, B.; Gschwend, O.; Carleton, A. Temporal coding in olfaction. In: Menini, A., editor. The Neurobiology of Olfaction. Boca Raton, FL: CRC Press/Taylor & Francis; 2010.

Bergmann O, Liebl J, Bernard S, Alkass K, Yeung MS, Steier P, Kutschera W, Johnson L, Landén M, Druid H, et al. The age of olfactory bulb neurons in humans. Neuron. 2012; 74:634–639. [PubMed: 22632721]

Beshel J, Kopell N, Kay LM. Olfactory bulb gamma oscillations are enhanced with task demands. J Neurosci. 2007; 27:8358–8365. [PubMed: 17670982]

Bhalla US, Bower JM. Multiday recordings from olfactory bulb neurons in awake freely moving rats: spatially and temporally organized variability in odorant response properties. J Comput Neurosci. 1997; 4:221–256. [PubMed: 9257234]

Bisulco S, Slotnick B. Olfactory discrimination of short chain fatty acids in rats with large bilateral lesions of the olfactory bulbs. Chem Senses. 2003; 28:361–370. [PubMed: 12826532]

Blumhagen F, Zhu P, Shum J, Schärer YP, Yaksi E, Deisseroth K, Friedrich RW. Neuronal filtering of multiplexed odour representations. Nature. 2011; 479:493–498. [PubMed: 22080956]

Boyd AM, Sturgill JF, Poo C, Isaacson JS. Cortical feedback control of olfactory bulb circuits. Neuron. 2012; 76:1161–1174. [PubMed: 23259951]

Briggs F, Usrey WM. Parallel processing in the corticogeniculate pathway of the macaque monkey. Neuron. 2009; 62:135–146. [PubMed: 19376073]

Briggs F, Usrey WM. Corticogeniculate feedback and visual processing in the primate. J Physiol. 2011; 589:33–40. [PubMed: 20724361]

Brivanlou IH, Warland DK, Meister M. Mechanisms of concerted firing among retinal ganglion cells. Neuron. 1998; 20:527–539. [PubMed: 9539126]

Buck L, Axel R. A novel multigene family may encode odorant receptors: a molecular basis for odor recognition. Cell. 1991; 65:175–187. [PubMed: 1840504]

Burns ME, Baylor DA. Activation, deactivation, and adaptation in vertebrate photoreceptor cells. Annu Rev Neurosci. 2001; 24:779–805. [PubMed: 11520918]

Butts DA, Weng C, Jin J, Yeh CI, Lesica NA, Alonso JM, Stanley GB. Temporal precision in the neural code and the timescales of natural vision. Nature. 2007; 449:92–95. [PubMed: 17805296]

Cajal S. Significación fisiológica de las expansiones protoplásmicas y nerviosas de las células de la substancia gris. Revista de Ciencias Médicas, Barcelona. 1891; 22(XVII):1–15. (Memoria leída en el Congreso Médico de Valencia. Sesión de 24 de junio de 1891 con cinco grabados).

Cajal S. Croonian Lecture: la fine structure des centres nerveux. Proc R Soc Lond. 1894; 55:444–468.

Cajal S. Estudios sobre la corteza cerebral humana. IV Estructura de la corteza cerebral olfativa del hombre y mamíferos. Trab Lab Invest Biol. 1901; 1:1–140.

Cajal, S. Textura del Sistema Nervioso del Hombre y de los Vertebrados. Madrid: Moya; 1904.

Cang J, Isaacson JS. In vivo whole-cell recording of odor-evoked synaptic transmission in the rat olfactory bulb. J Neurosci. 2003; 23:4108–4116. [PubMed: 12764098]

Cassenaer S, Laurent G. Conditional modulation of spike-timing-dependent plasticity for olfactory learning. Nature. 2012; 482:47–52. [PubMed: 22278062]

Chaput MA. Respiratory-phase-related coding of olfactory information in the olfactory bulb of awake freely-breathing rabbits. Physiol Behav. 1986; 36:319–324. [PubMed: 3961008]

Choi GB, Stettler DD, Kallman BR, Bhaskar ST, Fleischmann A, Axel R. Driving opposing behaviors with ensembles of piriform neurons. Cell. 2011; 146:1004–1015. [PubMed: 21925321]

Christie JM, Bark C, Hormuzdi SG, Helbig I, Monyer H, Westbrook GL. Connexin36 mediates spike synchrony in olfactory bulb glomeruli. Neuron. 2005; 46:761–772. [PubMed: 15924862]

Cleland TA. Early transformations in odor representation. Trends Neurosci. 2010; 33:130–139. [PubMed: 20060600]

Cleland TA, Sethupathy P. Non-topographical contrast enhancement in the olfactory bulb. BMC Neurosci. 2006; 7:7. [PubMed: 16433921]

Cury KM, Uchida N. Robust odor coding via inhalation-coupled transient activity in the mammalian olfactory bulb. Neuron. 2010; 68:570–585. [PubMed: 21040855]

Dan Y, Atick JJ, Reid RC. Efficient coding of natural scenes in the lateral geniculate nucleus: experimental test of a computational theory. J Neurosci. 1996; 16:3351–3362. [PubMed: 8627371]

Davison IG, Ehlers MD. Neural circuit mechanisms for pattern detection and feature combination in olfactory cortex. Neuron. 2011; 70:82–94. [PubMed: 21482358]

Davison IG, Katz LC. Sparse and selective odor coding by mitral/tufted neurons in the main olfactory bulb. J Neurosci. 2007; 27:2091–2101. [PubMed: 17314304]

De Carlos JA, López-Mascaraque L, Valverde F. Connections of the olfactory bulb and nucleus olfactorius anterior in the hedgehog (Erinaceus europaeus): fluorescent tracers and HRP study. J Comp Neurol. 1989; 279:601–618. [PubMed: 2918089]

Dhawale AK, Hagiwara A, Bhalla US, Murthy VN, Albeanu DF. Non-redundant odor coding by sister mitral cells revealed by light addressable glomeruli in the mouse. Nat Neurosci. 2010; 13:1404–1412. [PubMed: 20953197]

Doi E, Gauthier JL, Field GD, Shlens J, Sher A, Greschner M, Machado TA, Jepson LH, Mathieson K, Gunning DE, et al. Efficient coding of spatial information in the primate retina. J Neurosci. 2012; 32:16256–16264. [PubMed: 23152609]

Doucette W, Restrepo D. Profound context-dependent plasticity of mitral cell responses in olfactory bulb. PLoS Biol. 2008; 6:e258. [PubMed: 18959481]

Doucette W, Gire DH, Whitesell J, Carmean V, Lucero MT, Restrepo D. Associative cortex features in the first olfactory brain relay station. Neuron. 2011; 69:1176–1187. [PubMed: 21435561]

Eriksson PS, Perfilieva E, Björk-Eriksson T, Alborn AM, Nordborg C, Peterson DA, Gage FH. Neurogenesis in the adult human hippocampus. Nat Med. 1998; 4:1313–1317. [PubMed: 9809557]

Fang Y, Cho KS, Tchedre K, Woo Lee S, Guo C, Kinouchi H, Fried S, Sun X, Chen DF. Ephrin-A3 suppresses Wnt signaling to control retinal stem cell potency. Stem Cells. 2013; 31:349–359. [PubMed: 23165658]

Field GD, Chichilnisky EJ. Information processing in the primate retina: circuitry and coding. Annu Rev Neurosci. 2007; 30:1–30. [PubMed: 17335403]

Franks KM, Russo MJ, Sosulski DL, Mulligan AA, Siegelbaum SA, Axel R. Recurrent circuitry dynamically shapes the activation of piriform cortex. Neuron. 2011; 72:49–56. [PubMed: 21982368]

Friedrich RW, Habermann CJ, Laurent G. Multiplexing using synchrony in the zebrafish olfactory bulb. Nat Neurosci. 2004; 7:862–871. [PubMed: 15273692]

Fukunaga I, Berning M, Kollo M, Schmaltz A, Schaefer AT. Two distinct channels of olfactory bulb output. Neuron. 2012; 75:320–329. [PubMed: 22841316]

Ghatpande AS, Reisert J. Olfactory receptor neuron responses coding for rapid odour sampling. J Physiol. 2011; 589:2261–2273. [PubMed: 21486768]

Ghosh S, Larson SD, Hefzi H, Marnoy Z, Cutforth T, Dokka K, Baldwin KK. Sensory maps in the olfactory cortex defined by long-range viral tracing of single neurons. Nature. 2011; 472:217–220. [PubMed: 21451523]

Gire DH, Franks KM, Zak JD, Tanaka KF, Whitesell JD, Mulligan AA, Hen R, Schoppa NE. Mitral cells in the olfactory bulb are mainly excited through a multistep signaling path. J Neurosci. 2012; 32:2964–2975. [PubMed: 22378870]

Godfrey PA, Malnic B, Buck LB. The mouse olfactory receptor gene family. Proc Natl Acad Sci USA. 2004; 101:2156–2161. [PubMed: 14769939]

Gollisch T, Meister M. Rapid neural coding in the retina with relative spike latencies. Science. 2008; 319:1108–1111. [PubMed: 18292344]

Gollisch T, Meister M. Eye smarter than scientists believed: neural computations in circuits of the retina. Neuron. 2010; 65:150–164. [PubMed: 20152123]

Gourévitch B, Kay LM, Martin C. Directional coupling from the olfactory bulb to the hippocampus during a go/no-go odor discrimination task. J Neurophysiol. 2010; 103:2633–2641. [PubMed: 20164392]

Gschwend O, Beroud J, Carleton A. Encoding odorant identity by spiking packets of rate-invariant neurons in awake mice. PLoS ONE. 2012; 7:e30155. [PubMed: 22272291]

Haberly LB. Parallel-distributed processing in olfactory cortex: new insights from morphological and physiological analysis of neuronal circuitry. Chem Senses. 2001; 26:551–576. [PubMed: 11418502]

Hayar A, Shipley MT, Ennis M. Olfactory bulb external tufted cells are synchronized by multiple intraglomerular mechanisms. J Neurosci. 2005; 25:8197–8208. [PubMed: 16148227]

Hopfield JJ. Pattern recognition computation using action potential timing for stimulus representation. Nature. 1995; 376:33–36. [PubMed: 7596429]

Hurst JL, Beynon RJ. Scent wars: the chemobiology of competitive signalling in mice. Bioessays. 2004; 26:1288–1298. [PubMed: 15551272]

Igarashi KM, Ieki N, An M, Yamaguchi Y, Nagayama S, Kobayakawa K, Kobayakawa R, Tanifuji M, Sakano H, Chen WR, Mori K. Parallel mitral and tufted cell pathways route distinct odor information to different targets in the olfactory cortex. J Neurosci. 2012; 32:7970–7985. [PubMed: 22674272]

Illig KR. Projections from orbitofrontal cortex to anterior piriform cortex in the rat suggest a role in olfactory information processing. J Comp Neurol. 2005; 488:224–231. [PubMed: 15924345]

Imamura F, Ayoub AE, Rakic P, Greer CA. Timing of neurogenesis is a determinant of olfactory circuitry. Nat Neurosci. 2011; 14:331–337. [PubMed: 21297629]

Isaacson JS. Odor representations in mammalian cortical circuits. Curr Opin Neurobiol. 2010; 20:328–331. [PubMed: 20207132]

Johnson BA, Leon M. Chemotopic odorant coding in a mammalian olfactory system. J Comp Neurol. 2007; 503:1–34. [PubMed: 17480025]

Johnson DM, Illig KR, Behan M, Haberly LB. New features of connectivity in piriform cortex visualized by intracellular injection of pyramidal cells suggest that "primary" olfactory cortex functions like "association" cortex in other sensory systems. J Neurosci. 2000; 20:6974–6982. [PubMed: 10995842]

Kay LM, Laurent G. Odor- and context-dependent modulation of mitral cell activity in behaving rats. Nat Neurosci. 1999; 2:1003–1009. [PubMed: 10526340]

Kay LM, Beshel J, Brea J, Martin C, Rojas-Líbano D, Kopell N. Olfactory oscillations: the what, how and what for. Trends Neurosci. 2009; 32:207–214. [PubMed: 19243843]

Kesner RP, Hunsaker MR, Ziegler W. The role of the dorsal and ventral hippocampus in olfactory working memory. Neurobiol Learn Mem. 2011; 96:361–366. [PubMed: 21742047]

Kwak J, Willse A, Matsumura K, Curran Opiekun M, Yi W, Preti G, Yamazaki K, Beauchamp GK. Genetically-based olfactory signatures persist despite dietary variation. PLoS ONE. 2008; 3:e3591. [PubMed: 18974891]

Kwak J, Willse A, Preti G, Yamazaki K, Beauchamp GK. In search of the chemical basis for MHC odourtypes. Proc Biol Sci. 2010; 277:2417–2425. [PubMed: 20356897]

Laughlin SB. Energy as a constraint on the coding and processing of sensory information. Curr Opin Neurobiol. 2001; 11:475–480. [PubMed: 11502395]

Laughlin SB, Sejnowski TJ. Communication in neuronal networks. Science. 2003; 301:1870–1874. [PubMed: 14512617]

Laurent G. Olfactory network dynamics and the coding of multidimensional signals. Nat Rev Neurosci. 2002; 3:884–895. [PubMed: 12415296]

Levy WB, Baxter RA. Energy efficient neural codes. Neural Comput. 1996; 8:531–543. [PubMed: 8868566]

Linster C, Cleland TA. Glomerular microcircuits in the olfactory bulb. Neural Netw. 2009; 22:1169–1173. [PubMed: 19646847]

Lopez-Mascaraque, L. Santiago Ramón y Cajal-Cien Años después Chemoreception. Madrid: Ediciones Piramide; 2006. La vía olfatoria: el error de Cajal; p. 213-221.

Lowe G. Electrical signaling in the olfactory bulb. Curr Opin Neurobiol. 2003; 13:476–481. [PubMed: 12965296]

Luna VM, Schoppa NE. GABAergic circuits control input-spike coupling in the piriform cortex. J Neurosci. 2008; 28:8851–8859. [PubMed: 18753387]

Ma, M. Multiple olfactory subsystems convey various sensory signals. In: Menini, A., editor. The Neurobiology of Olfaction. Boca Raton, FL: CRC Press/ Taylor & Francis; 2010.

Maier JX, Wachowiak M, Katz DB. Chemosensory convergence on primary olfactory cortex. J Neurosci. 2012; 32:17037–17047. [PubMed: 23197697]

Margrie TW, Schaefer AT. Theta oscillation coupled spike latencies yield computational vigour in a mammalian sensory system. J Physiol. 2003; 546:363–374. [PubMed: 12527724]

Markopoulos F, Rokni D, Gire DH, Murthy VN. Functional properties of cortical feedback projections to the olfactory bulb. Neuron. 2012; 76:1175–1188. [PubMed: 23259952]

Martin C, Gervais R, Hugues E, Messaoudi B, Ravel N. Learning modulation of odor-induced oscillatory responses in the rat olfactory bulb: a correlate of odor recognition? J Neurosci. 2004; 24:389–397. [PubMed: 14724237]

Matsutani S. Trajectory and terminal distribution of single centrifugal axons from olfactory cortical areas in the rat olfactory bulb. Neuroscience. 2010; 169:436–448. [PubMed: 20457224]

Ming GL, Song H. Adult neurogenesis in the mammalian central nervous system. Annu Rev Neurosci. 2005; 28:223–250. [PubMed: 16022595]

Miura K, Mainen ZF, Uchida N. Odor representations in olfactory cortex: distributed rate coding and decorrelated population activity. Neuron. 2012; 74:1087–1098. [PubMed: 22726838]

Miyamichi K, Amat F, Moussavi F, Wang C, Wickersham I, Wall NR, Taniguchi H, Tasic B, Huang ZJ, He Z, et al. Cortical representations of olfactory input by trans-synaptic tracing. Nature. 2011; 472:191–196. [PubMed: 21179085]

Mori K, Sakano H. How is the olfactory map formed and interpreted in the mammalian brain? Annu Rev Neurosci. 2011; 34:467–499. [PubMed: 21469960]

Mori K, Shepherd GM. Emerging principles of molecular signal processing by mitral/tufted cells in the olfactory bulb. Semin Cell Biol. 1994; 5:65–74. [PubMed: 8186397]

Mori K, Nagao H, Yoshihara Y. The olfactory bulb: coding and processing of odor molecule information. Science. 1999; 286:711–715. [PubMed: 10531048]

Mori K, Takahashi YK, Igarashi KM, Yamaguchi M. Maps of odorant molecular features in the Mammalian olfactory bulb. Physiol Rev. 2006; 86:409–433. [PubMed: 16601265]

Munger SD, Leinders-Zufall T, Zufall F. Subsystem organization of the mammalian sense of smell. Annu Rev Physiol. 2009; 71:115–140. [PubMed: 18808328]

Nagayama S, Takahashi YK, Yoshihara Y, Mori K. Mitral and tufted cells differ in the decoding manner of odor maps in the rat olfactory bulb. J Neurophysiol. 2004; 91:2532–2540. [PubMed: 14960563]

Nagayama S, Enerva A, Fletcher ML, Masurkar AV, Igarashi KM, Mori K, Chen WR. Differential axonal projection of mitral and tufted cells in the mouse main olfactory system. Front Neural Circuits. 2010; 4:120. [PubMed: 20941380]

Najac M, De Saint Jan D, Reguero L, Grandes P, Charpak S. Monosynaptic and polysynaptic feed-forward inputs to mitral cells from olfactory sensory neurons. J Neurosci. 2011; 31:8722–8729. [PubMed: 21677156]

Nakashima M, Mori K, Takagi SF. Centrifugal influence on olfactory bulb activity in the rabbit. Brain Res. 1978; 154:301–306. [PubMed: 687996]

Nara K, Saraiva LR, Ye X, Buck LB. A large-scale analysis of odor coding in the olfactory epithelium. J Neurosci. 2011; 31:9179–9191. [PubMed: 21697369]

Neville, KR.; Haberly, LB. Olfactory cortex. In: Shepherd, GM.; Greer, CA., editors. The Synaptic Organization of the Brain. New York: Oxford University Press; 2004. p. 415-454.

Nirenberg S, Pandarinath C. Retinal prosthetic strategy with the capacity to restore normal vision. Proc Natl Acad Sci USA. 2012; 109:15012–15017. [PubMed: 22891310]

Olshausen BA, Field DJ. Natural image statistics and efficient coding. Network. 1996; 7:333–339. [PubMed: 16754394]

Olshausen BA, Field DJ. Sparse coding of sensory inputs. Curr Opin Neurobiol. 2004; 14:481–487. [PubMed: 15321069]

Pager J. Respiration and olfactory bulb unit activity in the unrestrained rat: statements and reappraisals. Behav Brain Res. 1985; 16:81–94. [PubMed: 4041216]

Panzeri S, Brunel N, Logothetis NK, Kayser C. Sensory neural codes using multiplexed temporal scales. Trends Neurosci. 2010; 33:111–120. [PubMed: 20045201]

Poo C, Isaacson JS. Odor representations in olfactory cortex: "sparse" coding, global inhibition, and oscillations. Neuron. 2009; 62:850–861. [PubMed: 19555653]

Pressler RT, Strowbridge BW. Blanes cells mediate persistent feedforward inhibition onto granule cells in the olfactory bulb. Neuron. 2006; 49:889–904. [PubMed: 16543136]

Richard MB, Taylor SR, Greer CA. Age-induced disruption of selective olfactory bulb synaptic circuits. Proc Natl Acad Sci USA. 2010; 107:15613–15618. [PubMed: 20679234]

Rinberg D, Koulakov A, Gelperin A. Sparse odor coding in awake behaving mice. J Neurosci. 2006; 26:8857–8865. [PubMed: 16928875]

Rolls ET, Treves A, Tovee MJ, Panzeri S. Information in the neuronal representation of individual stimuli in the primate temporal visual cortex. J Comput Neurosci. 1997; 4:309–333. [PubMed: 9427118]

Royet JP, Souchier C, Jourdan F, Ploye H. Morphometric study of the glomerular population in the mouse olfactory bulb: numerical density and size distribution along the rostrocaudal axis. J Comp Neurol. 1988; 270:559–568. [PubMed: 3372747]

Saito H, Chi Q, Zhuang H, Matsunami H, Mainland JD. Odor coding by a Mammalian receptor repertoire. Sci Signal. 2009; 2:ra9. [PubMed: 19261596]

Salcedo E, Zhang C, Kronberg E, Restrepo D. Analysis of training-induced changes in ethyl acetate odor maps using a new computational tool to map the glomerular layer of the olfactory bulb. Chem Senses. 2005; 30:615–626. [PubMed: 16141292]

Schaefer AT, Margrie TW. Spatiotemporal representations in the olfactory system. Trends Neurosci. 2007; 30:92–100. [PubMed: 17224191]

Schaefer ML, Yamazaki K, Osada K, Restrepo D, Beauchamp GK. Olfactory fingerprints for major histocompatibility complex-determined body odors II: relationship among odor maps, genetics, odor composition, and behavior. J Neurosci. 2002; 22:9513–9521. [PubMed: 12417675]

Schoppa NE, Urban NN. Dendritic processing within olfactory bulb circuits. Trends Neurosci. 2003; 26:501–506. [PubMed: 12948662]

Shepherd, GM.; Chen, WR.; Greer, CA. Olfactory bulb. In: Shepherd, GM., editor. The Synaptic Organization of the Brain. New York: Oxford University Press; 2004. p. 159-204.

Shusterman R, Smear MC, Koulakov AA, Rinberg D. Precise olfactory responses tile the sniff cycle. Nat Neurosci. 2011; 14:1039–1044. [PubMed: 21765422]

Sincich LC, Horton JC, Sharpee TO. Preserving information in neural transmission. J Neurosci. 2009; 29:6207–6216. [PubMed: 19439598]

Slotnick B, Bodyak N. Odor discrimination and odor quality perception in rats with disruption of connections between the olfactory epithelium and olfactory bulbs. J Neurosci. 2002; 22:4205–4216. [PubMed: 12019338]

Smear M, Shusterman R, O'Connor R, Bozza T, Rinberg D. Perception of sniff phase in mouse olfaction. Nature. 2011; 479:397–400. [PubMed: 21993623]

Sosulski DL, Bloom ML, Cutforth T, Axel R, Datta SR. Distinct representations of olfactory information in different cortical centres. Nature. 2011; 472:213–216. [PubMed: 21451525]

Soucy ER, Albeanu DF, Fantana AL, Murthy VN, Meister M. Precision and diversity in an odor map on the olfactory bulb. Nat Neurosci. 2009; 12:210–220. [PubMed: 19151709]

Spors H, Wachowiak M, Cohen LB, Friedrich RW. Temporal dynamics and latency patterns of receptor neuron input to the olfactory bulb. J Neurosci. 2006; 26:1247–1259. [PubMed: 16436612]

Sterling, P.; Demb, JB. Retina. In: Shepherd, GM., editor. The Synaptic Organization of the Brain. New York: Oxford University Press; 2004. p. 217-270.

Stokes CC, Isaacson JS. From dendrite to soma: dynamic routing of inhibition by complementary interneuron microcircuits in olfactory cortex. Neuron. 2010; 67:452–465. [PubMed: 20696382]

Strowbridge BW. Role of cortical feedback in regulating inhibitory microcircuits. Ann N Y Acad Sci. 2009; 1170:270–274. [PubMed: 19686146]

Sur M, Garraghty PE, Roe AW. Experimentally induced visual projections into auditory thalamus and cortex. Science. 1988; 242:1437–1441. [PubMed: 2462279]

Suzuki N, Bekkers JM. Microcircuits mediating feedforward and feedback synaptic inhibition in the piriform cortex. J Neurosci. 2012; 32:919–931. [PubMed: 22262890]

Vanderwolf CH. Hippocampal activity, olfaction, and sniffing: an olfactory input to the dentate gyrus. Brain Res. 1992; 593:197–208. [PubMed: 1450928]

Vincis R, Gschwend O, Bhaukaurally K, Beroud J, Carleton A. Dense representation of natural odorants in the mouse olfactory bulb. Nat Neurosci. 2012; 15:537–539. [PubMed: 22406552]

Wachowiak M, Shipley MT. Coding and synaptic processing of sensory information in the glomerular layer of the olfactory bulb. Semin Cell Dev Biol. 2006; 17:411–423. [PubMed: 16765614]

Wang HP, Spencer D, Fellous JM, Sejnowski TJ. Synchrony of thalamocortical inputs maximizes cortical reliability. Science. 2010; 328:106–109. [PubMed: 20360111]

Wilson DA. Scopolamine enhances generalization between odor representations in rat olfactory cortex. Learn Mem. 2001; 8:279–285. [PubMed: 11584075]

Wilson M, Lindstrom SH. What the bird's brain tells the bird's eye: the function of descending input to the avian retina. Vis Neurosci. 2011; 28:337–350. [PubMed: 21524338]

Wilson, DA.; Rennaker, RL. Cortical activity evoked by odors. In: Menini, A., editor. The Neurobiology of Olfaction. Boca Raton, FL: CRC Press/ Taylor & Francis; 2010.

Wilson DA, Sullivan RM. Cortical processing of odor objects. Neuron. 2011; 72:506–519. [PubMed: 22099455]

Wilson DA, Best AR, Brunjes PC. Trans-neuronal modification of anterior piriform cortical circuitry in the rat. Brain Res. 2000; 853:317–322. [PubMed: 10640629]

Xu W, Wilson DA. Odor-evoked activity in the mouse lateral entorhinal cortex. Neuroscience. 2012; 223:12–20. [PubMed: 22871522]

Zhang X, Firestein S. The olfactory receptor gene superfamily of the mouse. Nat Neurosci. 2002; 5:124–133. [PubMed: 11802173]

Zhao C, Deng W, Gage FH. Mechanisms and functional implications of adult neurogenesis. Cell. 2008; 132:645–660. [PubMed: 18295581]

Zhou Z, Belluscio L. Coding odorant concentration through activation timing between the medial and lateral olfactory bulb. Cell Rep. 2012; 2:1143–1150. [PubMed: 23168258]
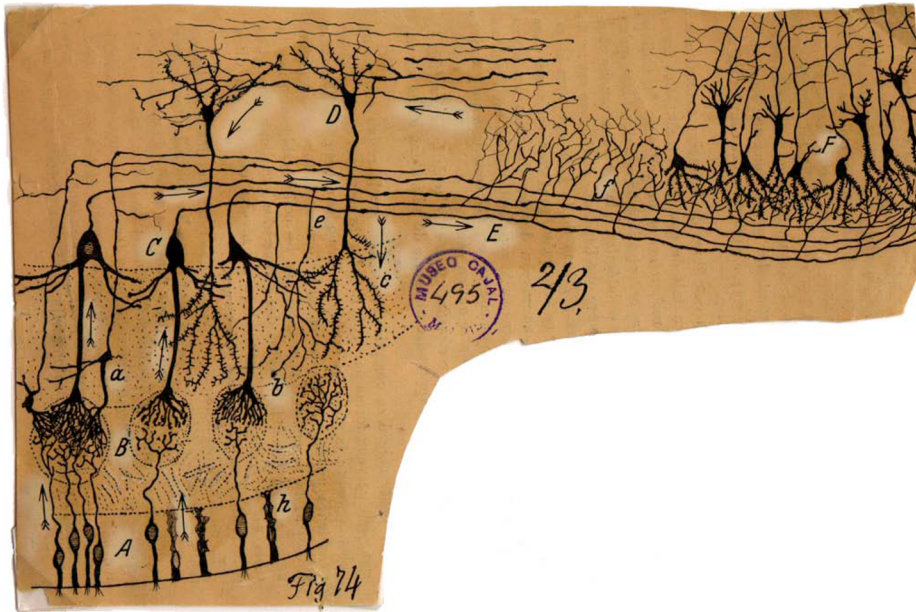
Figure 1. Cajal's Scheme Showing the Neuronal Connections and Signal Flow (Arrows) in the Olfactory System

Scheme (Cajal, 1891) of cellular connections of the olfactory mucosa, olfactory bulb, tractus, and olfactory lobe (piriform cortex) of the brain. The arrows indicate the direction of signaling. (A) Bipolar olfactory sensory neurons of the olfactory epithelium; (B) glomeruli; (C) mitral cells; (D) granule cells; (E) external root (lateral olfactory tract); (F) sphenoidal, piriform cortex; (a) small tufted cell; (b) apical dendrite of a mitral cell; (c) terminal ramification of a granule cell; (e) mitral cell recurrent ramifications; (h) epithelial sustentacular cells in the olfactory mucosa (Cajal, 1894). Reprinted with permission of Cajal Legacy, Instituto Cajal, CSIC, Madrid.
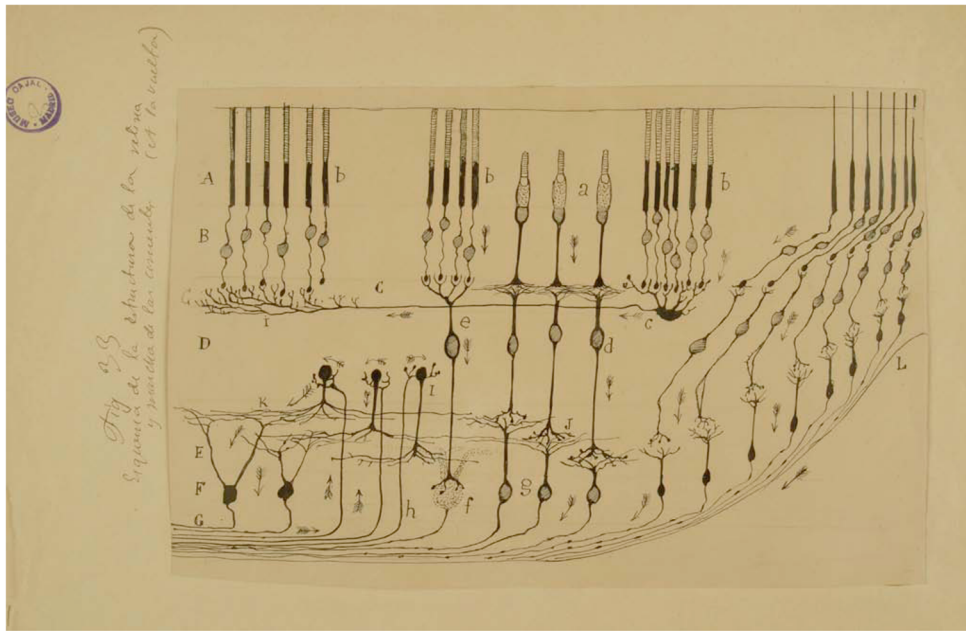
Figure 2. Cajal's Diagram Showing the Layers, Cell Types, Connections, and Signal Flow (Arrows) in the Avian Retina (Cajal, 1891) Where There Is Significant Centrifugal Feedback (Wilson and Lindstrom, 2011)

(A) Layer of rods and cones (photoreceptors); (B) visual cell body layer; (C) external plexiform layer; (D) bipolar cell layer; (E) inner plexiform layer; (F) ganglion cell layer; (G) optic nerve fiber layer. Arrows symbolize the flow of information from the photoreceptor cells to intermediary layers of neurons that locally process visual information before it is sent to higher areas in the brain (Cajal, 1901). Reprinted with permission of Cajal Legacy, Instituto Cajal, CSIC, Madrid.
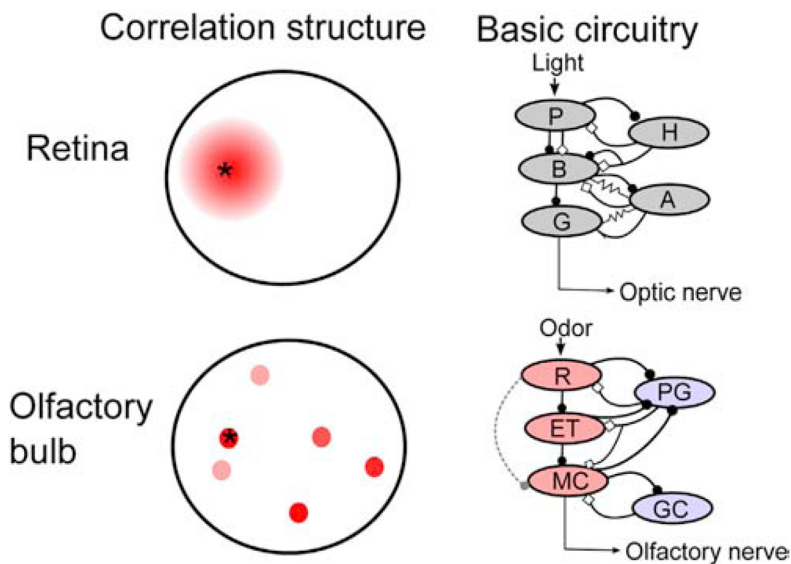
Figure 3. Current Understanding of the Basic Properties of the Olfactory Bulb and Retina
Left panel: correlation structure of input to the retina (top) and olfactory bulb (bottom). Red indicates the degree of correlated input relative to the indicated point (asterisk). In the retina, neighboring circuits of neurons receive similar information, allowing for center surround inhibition and other local computations to be performed. The olfactory bulb, due to the high number of different receptor types, cannot map its input onto a two-dimensional surface, and so olfactory input is necessarily fragmented across the olfactory bulb (Cleland and Sethupathy, 2006), and nearby glomeruli do not receive correlated input (Soucy et al., 2009). Right panel: basic circuit diagrams of modular networks within the retina (top, after Gollisch and Meister, 2010) and olfactory bulb (bottom). Excitation is marked by closed circles and inhibition by open diamonds. Recent work suggests that transmission through the olfactory bulb may be more similar to the retina than previously thought, with external tufted (ET) cells acting as intermediaries between receptor neuron input (R) and mitral cell (MC) output, much as bipolar cells (B) function between photoreceptors (P) and retinal ganglion cells (G), although weak connections between the olfactory receptor neurons and MCs are also thought to exist (dashed line); understanding the relative functional contributions of these two pathways will require future work in awake animals. Periglomerular (PG) and granule cells (GC) provide inhibitory feedback onto ETs and MCs, functioning somewhat like horizontal (H) and amacrine (A) cells, although gap junctions have not been physiologically demonstrated between inhibitory and excitatory neurons in the olfactory bulb. Red cells are glutamatergic and blue GABAergic in the lower panel. Tufted cells, which share some properties with both MCs and ETs, are not shown.
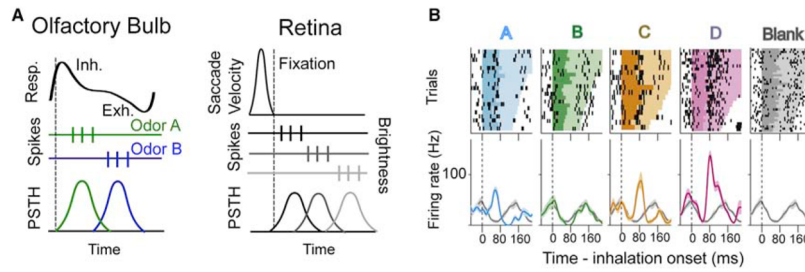
Figure 4. Spike Latency and Phase Coding during Active Sensing in the Olfactory Bulb and Retina

(A) Temporal codes in the olfactory bulb are computed relative to the onset of inhalation (dashed line). The top trace represents the breathing cycle, with upward deflection indicating inhalation (inh.) and downward exhalation (exh.). The timing of spikes (middle panel) relative to inhalation is informative regarding odor identity (peristimulus time histogram [PSTH] at bottom). In the retina, a similar temporal code set to the onset of fixation following a saccade has been suggested to efficiently convey stimulus information (Gollisch and Meister, 2008), with retinal ganglion cells having receptive fields in dark areas responding early (top spikes) and those in light areas responding later (bottom spikes). (B) Extracellular recordings from MT cells in the olfactory bulb of an awake rat (reproduced from Cury and Uchida, 2010) showing that alignment of spikes to inhalation (dashed line) is informative regarding the identity of an odor (A–D, distinct odors; blank is no odor). Top plots are raster plots with the duration of the sniff cycle indicated by color, and bottom plots are PSTHs with the Blank PSTH provided for reference in each plot.
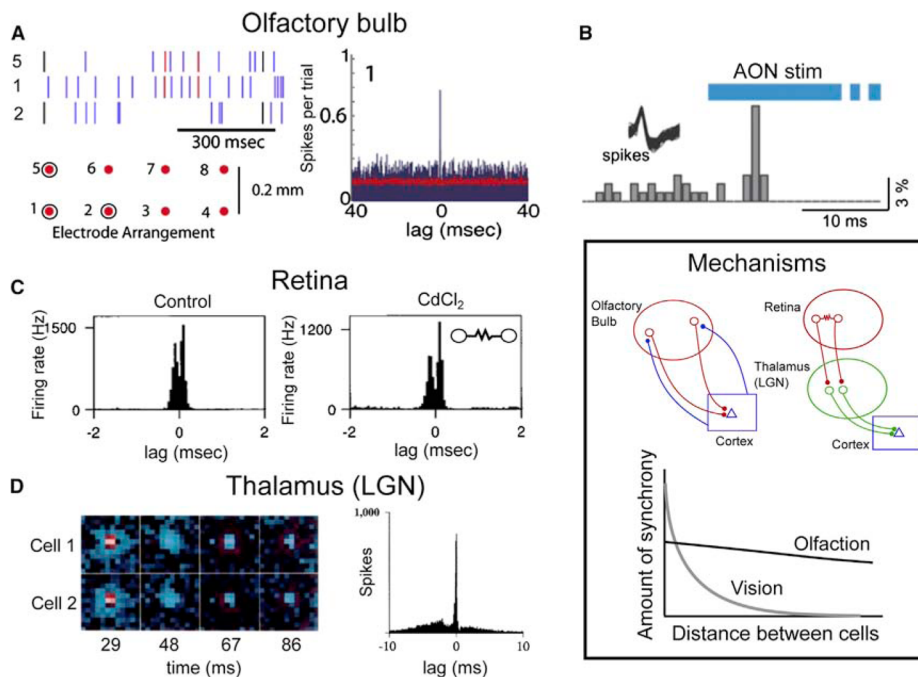
Figure 5. Precise Spike Timing and Synchrony in Vision and Olfaction

(A) Left panel: spikes recorded from mitral and tufted cells located >200 µm apart in the olfactory bulb show precise synchrony. Each spike train is from a unit recorded on the indicated lead (diagram below, with displayed leads circled) and spikes synchronized between units from leads 5 and 1 are colored red, those between 1 and 2 black. Right panel: lag histogram for units recorded from leads 5 and 1. Precise synchrony is evident as a peak near zero lag. Reproduced from (Doucette et al., 2011).

(B) Channelrhodopsin-2 activation following viral transduction of neurons in the anterior olfactory nucleus (AON, an olfactory cortical structure) results in precisely timed spikes in mitral and tufted cells, shown here as a sharp peak in firing after cortical feedback stimulation (reproduced from Markopoulos et al., 2012).

(C) Precise synchrony in the retina. Left panel: lag histogram demonstrating that retinal ganglion cells exhibit precise, submillisecond synchrony (note the timescale for the lag). Right panel: this synchrony is due to gap-junction mediated transmission between neighboring cells, as synaptic transmission block with cadmium fails to eliminate synchrony (inset is a diagram of the mechanism, resistor symbol indicates a gap junction between the two cells; reproduced from (Brivanlou et al., 1998)).

(D) Precise synchrony in the visual thalamus (lateral geniculate nucleus, LGN). Nearby cells with overlapping receptive fields (two ON cells in this case, receptive fields shown in the left panel) show precise synchrony, demonstrated in the lag histogram in the right panel. Reproduced from (Alonso et al., 1996). Inset: Mechanisms. While both the olfactory and visual systems employ precise synchrony, the mechanisms through which this synchrony arises are dictated by the demands of each system. Top panel (left): a plausible mechanism to support precise synchrony in the olfactory system. Common input from cortical feedback projections causes precisely synchronized spikes in olfactory bulb mitral and tufted cells. This mechanism does not rely on local connections within the olfactory bulb and would support synchrony that is observed at large distances across the olfactory bulb (bottom panel, solid line). Top panel (right): in contrast, the visual system generates precise synchrony through local interactions in the retina (gap junctions and common cone input) and through common input from the retina to cells in the LGN. This synchrony is much

stronger than that observed in the olfactory system when neighboring cells are considered, though it is distance dependent, falling off sharply at distances beyond 50–100 µm (gray curve in the bottom panel).
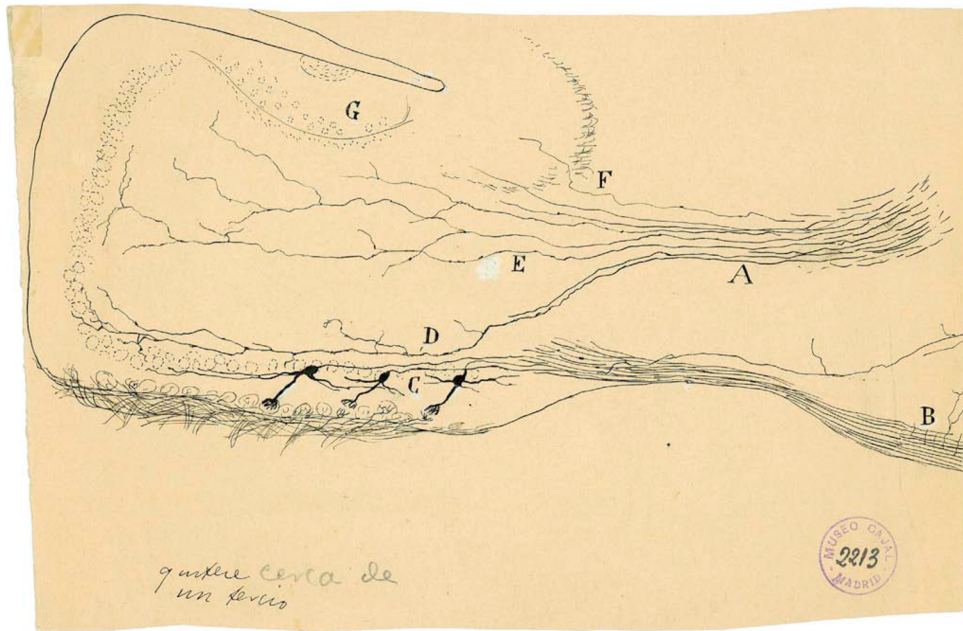
Figure 6. Cajal's Scheme Showing the Mitral Cell Centrifugal Innervation Visualized by Golgi Method in an 8-Day-Old Mouse
In this sagittal section A represents some afferent fibers from the anterior commissure ramifying in the granule cell layer. (A) anterior commissure; (B) external root of the olfactory bulb (lateral olfactory tract); (C) mitral cell layer; (D) axonal arborization restricted to the internal plexiform layer and the mitral cell layer; (E) afferent fibers from the anterior comissure with ramifications confined to the granule cell layer without entering into the mitral cell layer; (F) nonramified fibers may come from the cortex covered by the lateral olfactory tract ("corteza del pediculo bulbar"); (G) accessory olfactory bulb (Cajal, 1901). Reprinted with permission of Cajal Legacy, Instituto Cajal, CSIC, Madrid.
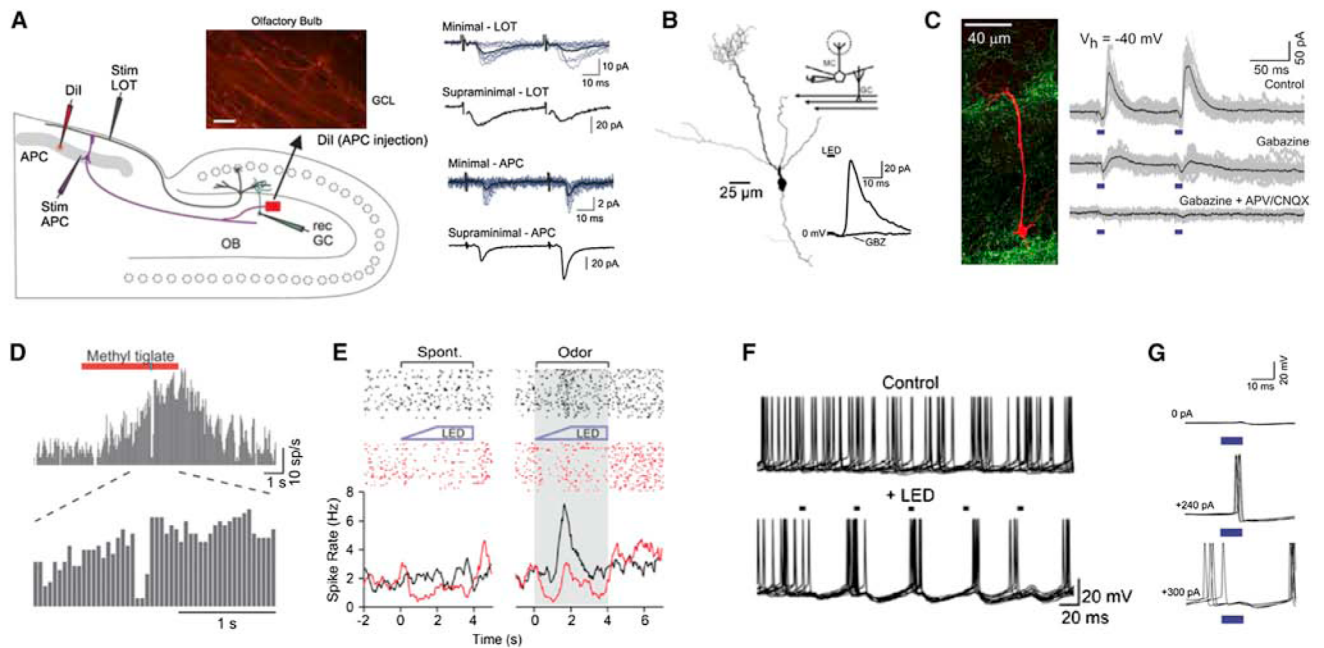
Figure 7. Functional Properties of Olfactory Corticofugal Feedback Projections

(A) Left panel: diagram of an experiment in a combined olfactory bulb/piriform cortex preparation. Stimulation was either directly to the anterior piriform cortex (Stim APC) or to the mitral cell axons (Stim LOT). Right panel: stimulation of piriform cortex feedback projections caused fast, facilitating EPSCs in inhibitory olfactory bulb granule cells. This form of excitation was different both in its kinetics and short-term plasticity when compared to mitral cell input to granule cells (LOT stim).

(B) Selective activation of APC terminals in the olfactory bulb (using viral transduction of neurons with a construct carrying ChR2) causes inhibition in mitral cells. This inhibition is blocked by application of the GABAa receptor antagonist, gabazine (inset trace).

(C) Selective activation of the AON using a similar strategy causes both monosynaptic excitation (blocked by glutamate antagonists) and disynaptic inhibition (blocked by gabazine) in mitral cells. In vivo, both AON (D) and APC (E) feedback activation inhibit mitral cell responses to odorants.

(F) APC activation causes precisely timed spikes in mitral cells recorded in slices through rebound activation following inhibition.

(G) Due to direct excitation of mitral cells by AON input, AON activation can cause precisely timed spikes in mitral cells that are held near spike threshold with injected current (middle trace). The amount of current injected into the mitral cell is indicated for each set of traces.

(A) Reproduced with permission from Balu et al. (2007); (B), (E), and (F) reproduced from Boyd et al. (2012); and (C), (D), and (G) from Markopoulos et al. (2012).
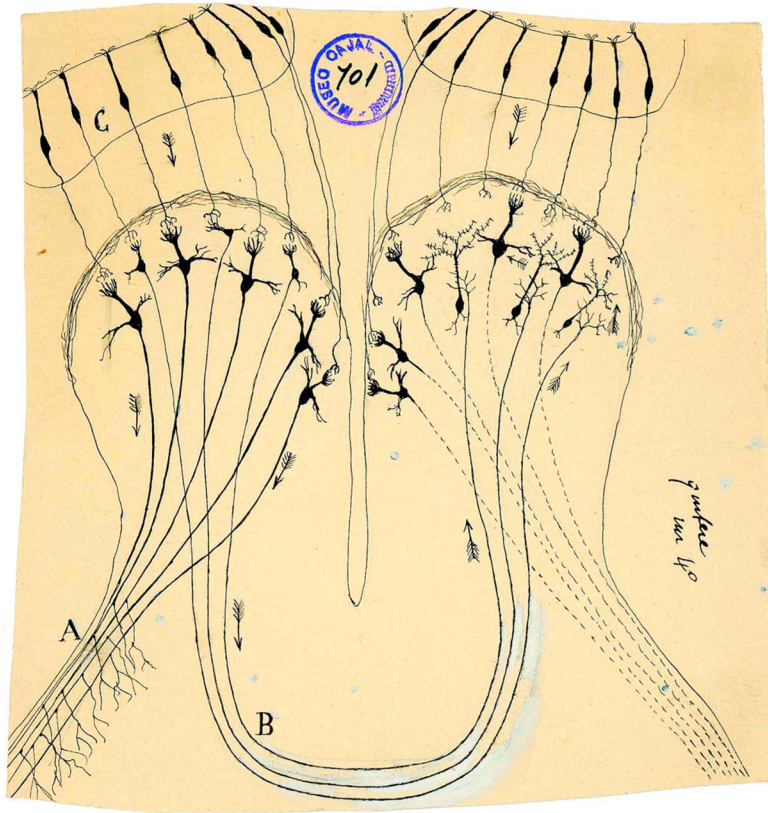
Figure 8. Drawing from Cajal Showing His *Incorrect* Conclusion that the Tufted Cells Send the Signals to the Contralateral Olfactory Bulb
(A) External root of the olfactory tract (lateral olfactory tract); (B) bulbar portion of the anterior commissure; (C) olfactory epithelium. Taken from (Cajal, 1901). Reprinted with permission of Cajal Legacy, Instituto Cajal, CSIC, Madrid.
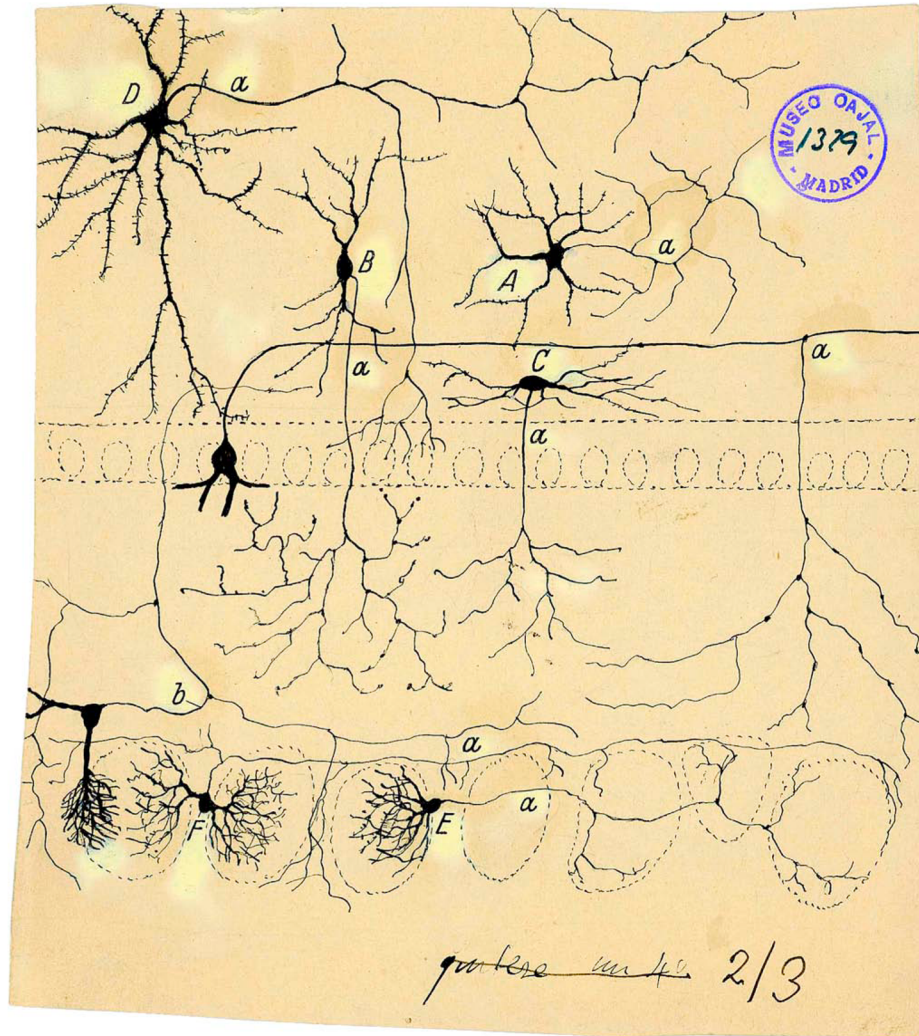
Figure 9. Cajal Drawing Showing Short Axon Cells in the Olfactory Bulb as Visualized in Golgi Preparations Performed by Cajal and His Pupil Blanes
(A) Golgi cell; (B) cell with peripheral axon; (C) fusiform horizontal cell of internal plexiform layer; (E and F) periglomerular cells; (a) axons; (b) axonal collateral from a tufted cell (Cajal, 1901). Reprinted with permission of Cajal Legacy, Instituto Cajal, CSIC, Madrid.
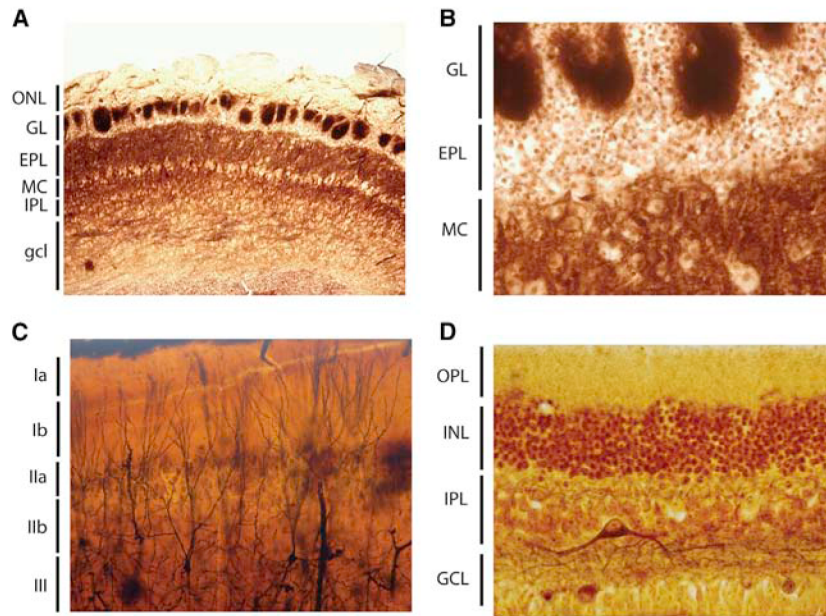
Figure 10. Histological Sections from Cajal of the Olfactory Bulb, Piriform Cortex, and the Retina

(A and B) Olfactory bulb from a rodent stained with a histological method to reveal fibers without myelin (probably the method of Del Rio Hortega). ONL, olfactory nerve layer; GL, glomerular layer; EPL, external plexiform layer; MC, mitral cell layer; IPL, internal plexiform layer; gcl, granule cell layer.

(C) Piriform cortex of the cat impregnated with the Golgi method. The different layers are layers Ia, Ib, IIa, IIb, and III. In the upper layer III appear impregnated some pyramidal cells sending their apical dendrites toward layer I, in whose thickness spread their terminal dendritic tufts.

(D) Retina from adult rabbit stained with the reduced silver nitrate method of Cajal. OPL, outer plexiform layer; INL, inner nuclear layer; IPL, inner plexiform layer; GCL ganglion cell layer.